Parameters affecting the electrical conductivity of SnO_2 : Sb sol–gel coatings

G. Gasparro, J. Pütz, D. Ganz, M.A. Aegerter*

Institut für Neue Materialien - INM, Department of Coating Technology, Im Stadtwald, Gebäude 43, D-66123 Saarbrücken, Germany

Abstract

SnO_2 : Sb single and multilayer coatings have been prepared by the sol–gel dip and spin coating method, and by spray pyrolysis from various precursor solutions. Subsequently, the films have been heat treated in a convection furnace or by cw CO_2 laser irradiation, respectively. The influence of the different deposition and heating techniques on the electrical and morphological properties of the resulting films has been investigated by van der Pauw/Hall method and high resolution transmission electron microscopy (HRTEM) cross-sectional images. It is shown that the resistivities of the dip and spin coated films are at least one order of magnitude higher compared to those of spray coated films obtained from the same precursor solution. In dip coated multilayer systems an alternating structure of loosely packed and dense layers can be observed leading to a decrease in resistivity with the number of layers. A similar densified surface structure is found in laser treated films together with larger crystallites. It is concluded that the differences in resistivity occurring from the deposition technique and the heating process are linked to structural differences of the coatings whereas the chemical composition of the solution plays a minor role for the electrical properties.

Keywords: Sol–gel; Thin film; SnO_2 : Sb; Electrical conductivity; Morphology

1. Introduction

Transparent electrically conducting coatings (TEC) deposited on glass are used today in a wide range of applications. The n-type semiconductor materials which

present the most interesting properties are indium tin oxide (ITO), fluorine or antimony-doped tin dioxide (FTO, ATO), tin oxide (TO) and zinc oxide (ZO) doped with Al (AZO), Ga (GZO), etc. Practically, all known coating processes have been used to deposit them on glass substrates. Transparent ITO and SnO_2 : F coatings prepared by sputtering and spray pyrolysis techniques, respectively, are now available commercially with sheet resistance as low as 5 $\Omega_{\square}$.

The sol–gel process [1] has been successfully applied for the preparation of ITO coatings [2–7]. Their electrical properties (resistivity ρ, carrier mobility μ, and carrier density n), and their optical properties (transmission and reflection in the visible and infrared range) are strongly dependent of the nature of the sols, the temperature, and atmosphere used during the sintering process. The lowest resistivities have always been obtained after sintering at relatively high temperatures (600°C or higher) and the best published value, $\rho = 1.8 \times 10^{-4}\ \Omega\,\text{cm}$ [5], is comparable to those typically obtained by other processes.

Few research works have been addressed to the preparation of sol–gel tin dioxide (TO) coatings. Most of the sols have been prepared from Sn(IV)-alkoxides such as Sn-ethoxide [8–10], Sn-propoxide [3,11], Sn-butoxide [12] or more complex systems [13,14]. $SnCl_4$ [15,16], Sn(II)-2-ethylhexanoate [17] and Sn(II)-citrate [18] have also been used. Antimony doping has been obtained by using $SbCl_3$ [15,19,20], $Sb(OEt)_3$ [9–11] and $Sb(OBu)_3$ [3,13,17] whereas fluorine doping has not yet been achieved with the sol-gel process. The use of sol stabilisers is only reported in [11,18].

The SnO_2 : Sb sol–gel coatings obtained until now present a relatively high resistivity, ranging typically from $\rho = 3 \times 10^{-3}\ \Omega\,\text{cm}$ [10] to $2.1 \times 10^{-2}\ \Omega\,\text{cm}$ [21]. The lowest value exceeds by more than an order of magnitude those obtained for coatings prepared by other methods (e. g. $\rho = 1 \times 10^{-5}\ \Omega\,\text{cm}$ for activated reactive evaporation of SnO_2 and SnO_2 : Sb [22] and $\rho = 2\text{–}6 \times 10^{-4}\ \Omega\,\text{cm}$ for spray pyrolysed SnO_2 : F films [23]).

The reasons for which the sol–gel process does not allow to obtain highly conductive SnO_2 films are still not clear. Chatelon et al. [9] observed a minimum in the films resistivity when the dip coating was performed in a 30–40% relative humidity and the film surface roughness was found to increase with the humidity. Spray pyrolysed SnO_2 : Sb coatings were found to exhibit a minimum in resistivity when the substrate temperature was 600°C [24]. The resistivity increases drastically when alkaline impurities are present in the coating and SiO_2 [21] or TiO_2 [11,21] buffer layers were found necessary if alkaline glasses or substrates are used. The crystallite size of sputtered coatings was found to increase both with the film thickness and temperature and to influence the resistivity [25].

This paper presents experimental results on the influence of the type of precursor and stabiliser and densification processes (furnace and laser treatment) on the electrical properties of single and multilayers SnO_2 : Sb prepared by dip or spin coating and by spray pyrolysis. When not noted all results have been obtained for coatings prepared from sols doped with 5 mol% Sb and heat treated at 550°C in air for 15 min.

2. Experimental

Single and multilayer sol–gel coatings have been obtained by dip and spin coating either on borosilicate glass or fused silica substrates. The coating solution used for dip coating contained 5 mol% $SbCl_3$ in a 0.5 M ethanolic solution of $SnCl_2(OAc)_2$. For spin deposition 0.2 M solutions of $Sn(O^tBu)_4$, $SnCl_4$, $SnCl_2(OAc)_2$, $Sn(OAc)_4$, $SnCl_2$, or Sn(II)-2-ethylhexanoate have been used without stabilisation or with an equimolar quantity of a stabiliser (L(+)-tartaric acid, succinic acid, citric acid, oxalic acid, triethanolamine, ethylenediamine, acetylacetone, diacetone alcohol) [26]. The sintering of the films was performed in air either in a furnace (dip and spin coated films) or by cw CO_2 laser irradiation (dip coated films) which is described elsewhere [27]. Coatings have also been obtained by spray pyrolysis on a 550°C preheated borosilicate substrate using the same solution of $SnCl_2(OAc)_2$ as described above. The electrical properties have been determined by Van der Pauw technique with a 0.3 T magnetic field. High resolution transmission electron microscopy (HRTEM) cross-sectional images were used to obtain information on the layer morphology. The coating thickness was measured with a Tencor P10 surface profiler.

3. Results and discussion

3.1. Influence of precursors and stabilisers

The influence of the chemical composition of the sol on the resistivity of the coatings, measured by the Van der Pauw technique, has been studied in detail [26]. Fig. 1 shows the values obtained for 40 nm thick films made from six sols either unstabilised or stabilised with (L +)-tartaric acid. The choice of the precursor and the fact that the sol is stabilised influence very strongly the electrical conductivity of the coatings. Fig. 2 shows the effect of different stabilisers on the resistivity of coatings made from $Sn(O^tBu)_4$ and $SnCl_4$ precursors, respectively. The correct choice of the stabiliser is essential for the $SnCl_4$-solution to obtain better resistivity values but has very little influence in the case of the alkoxide-based sol. This is due to the high chloride content of the first solution which leads to both volatile antimony and tin compounds. Hence part of the dopant and of the basic tin compounds are lost during the early stages of the firing process. Contrary, the alkoxide has to be stabilised only against uncontrolled hydrolysis.

The lowest resistivities are however never below $1 \times 10^{-2}\ \Omega$ cm, a value still ten times higher than that obtained for a film coated by spray pyrolysis using $SnCl_2(OAc)_2$ as precursor (Fig. 1). It is concluded that the deposition technique plays an important role and that the differences in resistivity are probably linked to structural differences of the coatings.

3.2. Influence of the deposition technique

TEM cross-section of spray and dip coated SnO_2 : Sb layers are shown in Figs. 3 and 4. Both layers reveal a totally different texture. The layer prepared by spray

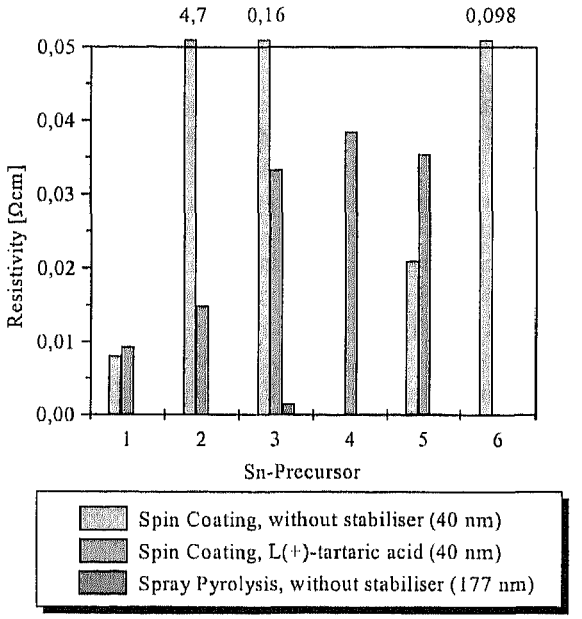

Fig. 1. Influence of the precursors and stabilisers on the resistivity of single layer SnO_2 : Sb coatings; 1: $Sn(O^tBu)_4$, 2: $SnCl_4$, 3: $SnCl_2(OAc)_2$, 4: $Sn(OAc)_4$, 5: $SnCl_2$, 6: Sn(II)-2-ethylhexanoate.

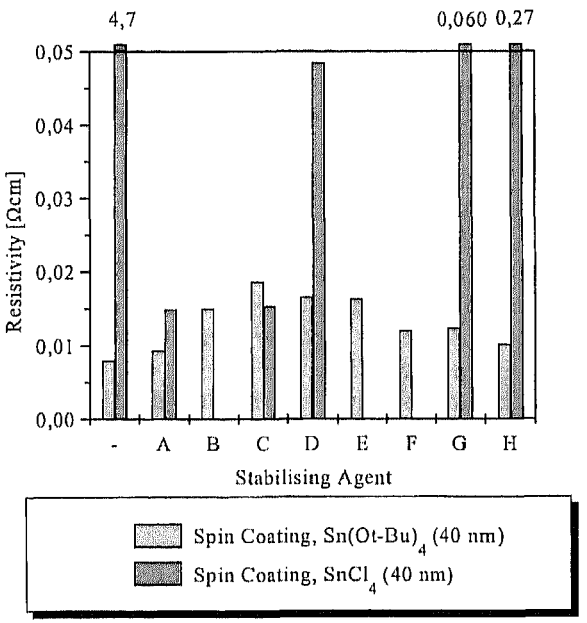

Fig. 2. Influence of the stabilisers on the resistivity of 40 nm thick single layer spin coated SnO_2 : Sb, heat treatment at 550°C for 15 min in air; (−) without stabiliser; (A) L(+)-tartaric acid, (B) succinic acid, (C) citric acid, (D) oxalic acid, (E) triethanolamine, (F) ethylene diamine, (G) acetylacetone, (H) diacetone alcohol.

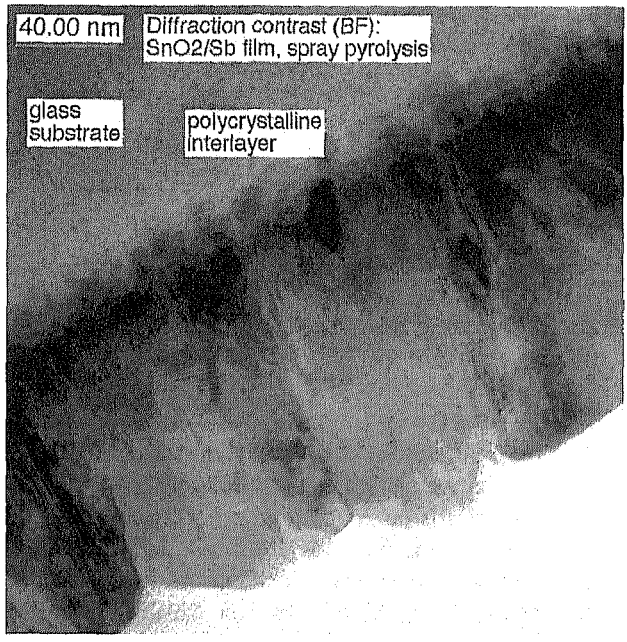

Fig. 3. TEM cross-section of a 177 nm thick sprayed SnO_2 : Sb coating.

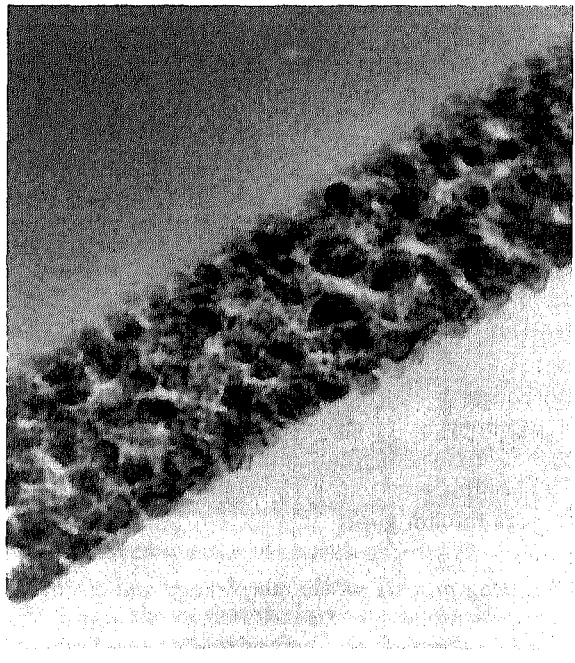

Fig. 4. TEM cross-section of a 70 nm thick dip coated single layer SnO_2 : Sb coating heat treated at 550°C for 15 min.

Table 1
Electrical parameters of SnO_2 : Sb layers prepared by different techniques from the same precursor $SnCl_2(OAc)_2$ (measured at 25°C) [27]

Technique	System	$n(cm^{-3})$	$\mu(cm^2/V\,s)$	$\rho(\Omega\,cm)$	$R(\Omega)$	Thickness (nm)
Furnace 550°C, 15 min	1 layer	2×10^{20}	1.7	1.5×10^{-2}	1300	110
Furnace 550°C, 15 min	10 layers	4×10^{20}	4.5	3.5×10^{-3}	130	260
CO_2 laser	1 layer	7.3×10^{20}	3.2	3.2×10^{-3}	250	120
Spray pyrolysis, 4 cycles	1 layer	4.2×10^{20}	9.7	1.5×10^{-3}	85	177

pyrolysis consists of large crystallites, densely packed in a columnar structure. It presents a rough and inhomogeneous surface. The morphology of a dip coated film is made of small, spherical shape crystallites that are loosely packed. Consequently the layer is porous but its surface is more homogeneous and smooth.

The electrical properties of the films are shown in Table 1. The higher electrical conductivity of spray coated films is certainly due to the presence of large and closely packed crystallites which allow a higher electron density and mobility. The small crystallite size and above all the porous structure observed in sol–gel dip coated single layers lead to lower n and μ values and consequently to a higher resistivity. On the other side the smooth surface and the small crystallite size observed in the dip coated sol–gel layers lead to minor light scattering effects and result in a higher optical transparency and a better optical appearance of the coatings than those obtained by spray pyrolysis where light scattering effects due to large crystallites and rougher surface affect the optical quality of the layers.

3.3. Influence of multiple coating

Fig. 5 shows the variation of the resistivity of coatings of same final thickness (200 nm) made by repeating the dip coated process several times (2–10 times). The resistivity is found to decrease with the number of layers. This phenomenon can be understood in terms of layer morphology as revealed by the TEM cross-sectional (Fig. 6).

The micrograph shows that the multilayer coatings are built of an alternating sequence of dense (top interface of each deposited layer) and porous material. For the same total thickness an increasing number of layers therefore increases the fraction of denser material in the film resulting in a smaller resistivity (Table 1). The optical properties of the layers remain good.

3.4. Influence of the firing process on the morphology and electrical parameters

The origin of the dense interface observed in Fig. 6 is not yet known. In order to test if the heating rate plays a role, single layer coatings have been sintered by using CO_2

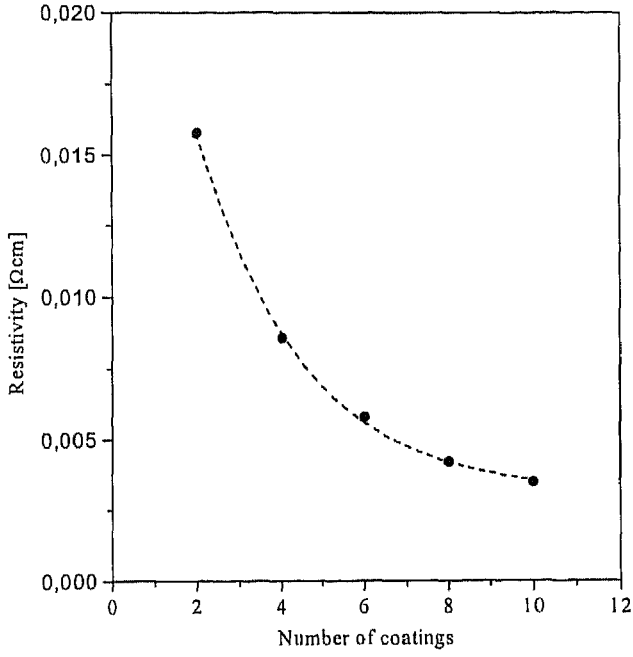

Fig. 5. Dependence of the resistivity on the number of layers, total coating thickness is the same (200 nm) for all results.

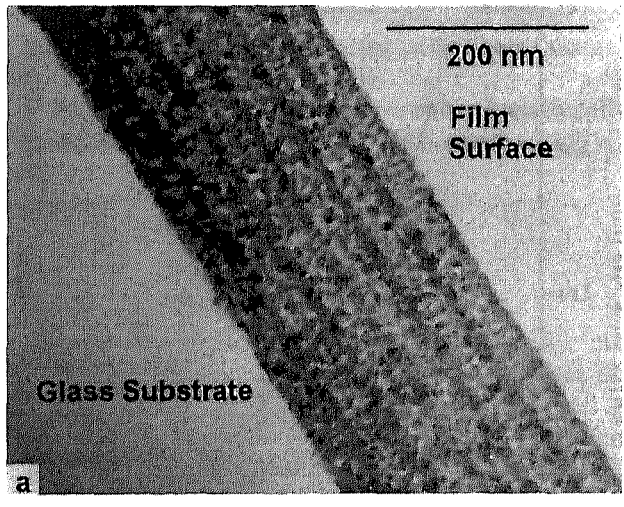

Fig. 6. TEM cross-section of a multilayer SnO_2 : Sb coating.

laser irradiation [27]. Fig. 7 shows that the layer thickness decreases with the applied laser energy density and X-ray reflectrometry and Rutherford Back Scattering (RBS) data have confirmed that this shrinkage is effectively due to a densification process.

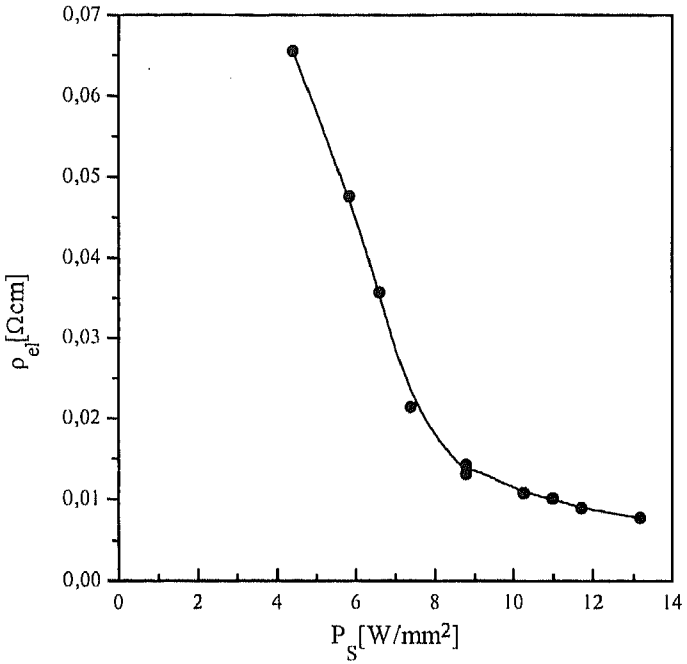

Fig. 7. Correlation between the laser power density and the resistivity of single layer SnO_2 : Sb coatings.

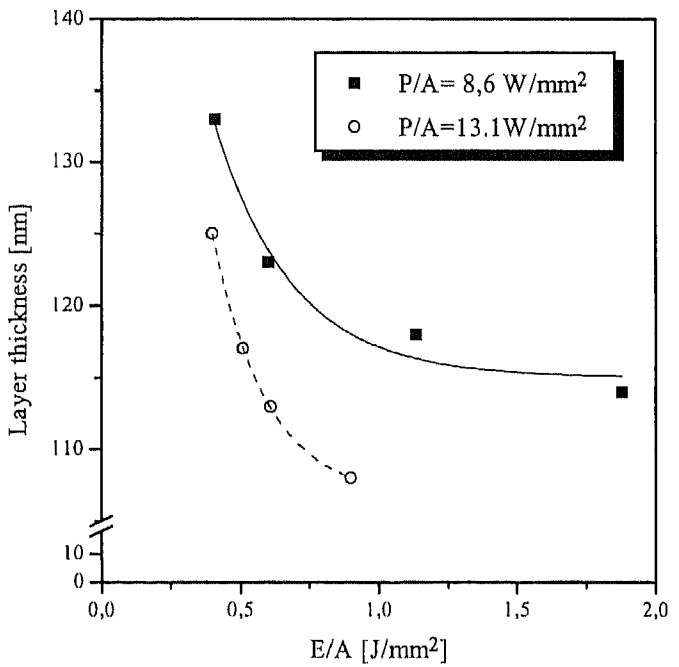

Fig. 8. Layer thickness of single layer SnO_2 : Sb coatings vs. CO_2 laser energy density.

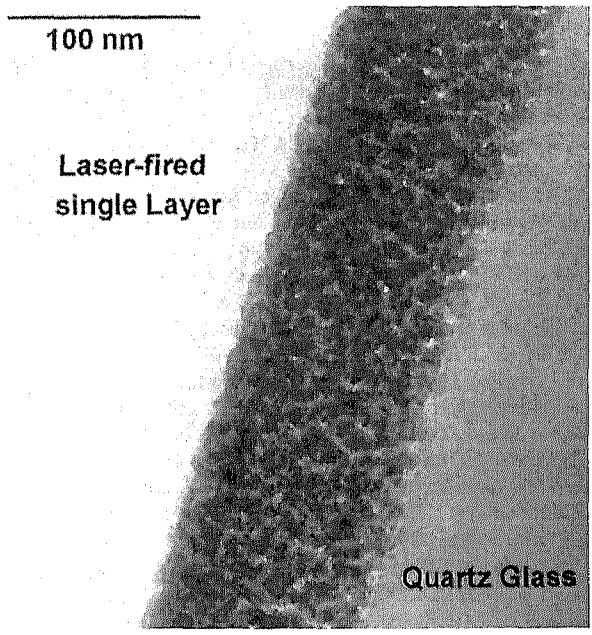

Fig. 9. TEM cross-section of a laser fired SnO_2 : Sb coating ($\rho = 3{,}2 \times 10^{-3}\ \Omega$ cm).

The resistivities of the layers decrease with increasing laser power density to a value four times lower than that obtained with a coating of the same thickness furnace fired at 550°C. (Fig. 8 and Table 1).

TEM cross-section (Fig. 9) shows that the layer is still made of small crystallites but packed in a denser texture and it is believed that this denser packing is responsible for the lower resistivity.

4. Conclusion

Transparent electrical conducting sol–gel SnO_2 : Sb coatings made by dip or spin-coating process present systematically higher resistivity values than those made by spray pyrolysis process. The type of precursor and stabiliser used for the preparation of the sol plays an important role. However the principal influence is probably due to the particular morphology of the layers. Contrary to spray-pyrolysed layers which consist of large, textured, densely packed particles arranged in a columnar structure, the sol–gel layers are built of small, almost spherical, loosely packed crystalline particles with a thin dense top interface. The overall morphology of single sol–gel layer sintered by CO_2 laser irradiation is similar but the film is made of larger and more densely packed particles. The resistivity is smaller by a factor 4. A decrease in the resistivity was also achieved when multilayers were deposited. For a constant thickness $\rho \sim 1/n$ were n is the number of layers.

References

[1] C.J. Brinker, G. Scherer, Sol-Gel Science, Academic Press, San Diego, 1990.
[2] N.J. Arfsten, R. Kaufmann, H. Dislich, German Patent DE 3300589 A 1, 1984.
[3] M. Mattox, Thin Solid Films 204 (1991) 25.
[4] T. Furusaki, K. Kodaira, in: P. Vincenzini (Ed.), High performance ceramic films and coatings, 241 Elsevier, Amsterdam, 1991.
[5] O. Yamamoto, T. Sasamoto, M. Inagaki, J. Mater. Res. 7 (1992) 2488.
[6] Y. Takahashi, H. Hayashi, Y. Ohya, Mater. Res. Soc. Symp. Proc. 271 (1992) 401.
[7] K. Nishio, T. Sei, T. Tsuchiya, J. Mater. Sci. 31 (1996) 1761.
[8] A. Maddalena, R. Del Machio, S. Diré, A. Raccanelli, J. Non-Cryst. Solids 121 (1990) 365.
[9] J.P. Chatelon, C. Terrier, E. Bernstein, R. Berjoan, J.A. Roger, Thin Solid Films 247 (1994) 162.
[10] C. Terrier, J.P. Chatelon, R. Berjoan, J.A. Roger, Thin Solid Films 263 (1995) 37.
[11] Y. Takahashi, Y. Wada, J. Electrochem. Soc. 137 (1990) 267.
[12] J.C. Giuntini, W. Granier, J.V. Zanchetta, A. Taha, J. Mater. Sci. Lett. 9 (1990) 1383.
[13] C.J.R. Gonzales-Oliver, I. Kato, J. Non-Cryst. Solids 82 (1986) 400.
[14] S.-S. Park, J.D. Mackenzie, Thin Solid Films 258 (1995) 268.
[15] D.E. Stilwell, S.-M. Park, J. Electrochem. Soc. 129 (1982) 1501.
[16] R.S. Hiratsuka, S.H. Pulcinelli, C.V. Santilli, J. Non-Cryst. Solids 121 (1990) 76.
[17] A. Tsunashima, H. Yoshimizu, K. Kodaira, S. Shimada, T. Matsushita, J. Mater. Sci. 21 (1986) 2731.
[18] P. Olivi, E.C. Pereira, E. Longo, J.A. Varella, L.O.S. Bulhoes, J. Electrochem. Soc. 140 (1993) L81.
[19] G. Gowda, D. Nguyen, Thin Solid Films 136 (1986) L39.
[20] B. Orel, U. Lavrencic-Stangar, Z. Crujak-Orel, P. Bukovec, M. Kosec, J. Non-Cryst. Solids 167 (1994) 272.
[21] W. Lada, A. Deptula, T. Olczak, W. Torbicz, D. Pijanowska, J. Sol-Gel Sci. Tech. 2 (1994) 551.
[22] H.S. Randhawa, M.D. Matthews, R.F. Bunshah, Thin Solid Films 83 (1981) 267.
[23] J. Dutta, J. Perrin, T. Emeraud, J.M. Laurent, A. Smith, J. Mater. Sci. 30 (1995) 53.
[24] H. Haitjema, Dissertation, Delft University, The Netherlands, 1989.
[25] D.J. Yoo, T. Tamaki, S.J. Park, N. Miura, N. Yamazoe, J. Electrochem. Soc. 142 (1995) L100.
[26] J. Pütz, Diploma Thesis, Universität des Saarlandes, Saarbrücken, Germany, 1996.
[27] D. Ganz, G. Gasparro, J. Otto, A. Reich, N.J. Arfsten, M.A. Aegerter, J. Mater. Sci. Lett. 16 (1997) 1233.